

Strain Effect on Energy Gaps of Armchair Graphene Nanoribbons

Lian Sun, Qunxiang Li, Hao Ren, Q. W. Shi, Jinlong Yang,* and J. G. Hou

Hefei National Laboratory for Physical Sciences at Microscale,

University of Science and Technology of China, Hefei, Anhui 230026, P.R. China

(Dated: April 5, 2019)

Abstract

We report a first-principles study on electronic structures of the deformed armchair graphene nanoribbons (AGNRs). The variation of the energy gap of AGNRs as a function of uniaxial strain displays a zigzag pattern, which indicates that the energy gaps of AGNRs can be effectively tuned. The spatial distributions of two occupied and two empty subbands close to the Fermi level are swapped under different strains. The tunable width of energy gaps becomes narrower as increasing the width of AGNRs. Our simulations with tight binding approximation, including the nearest neighbor hopping integrals between π - orbitals of carbon atoms, reproduce these results by first-principles calculations. One simple empirical formula is obtained to describe the scaling behavior of the maximal value of energy gap as a function of the width of AGNRs.

PACS numbers: 73.22.-f, 73.61.Wp

Nanoscale carbon materials including fullerenes and carbon nanotubes have attracted a great deal of research interest owing to its versatile electronic properties.^{1,2} Among them, graphene fabricated by Novoselov *et al.* firstly has been studied extensively.³ Many interesting properties of this kind layered two-dimensional carbon nanostructure, such as the Landau quantization,⁴ the integer quantum-Hall effect,^{5,6,7,8} and the quantization minimum conductivity,⁹ have been investigated by several experimental and theoretical research groups. Now much attention has focused on graphene nanoribbons (GNRs) with various widths, which can be realized by cutting the exfoliated graphene, or by patterning graphene epitaxially.^{8,10,11} The edge carbon atoms of graphene ribbons have two typical topological shapes: namely armchair and zigzag. All zigzag graphene nanoribbons (ZGNR) are metallic due to a localized state at the Fermi level. This has been confirmed by scanning tunneling spectroscopy and atomic force microscopy.^{12,13,14} It originates from a gauge field produced by lattice deformation. Such a localized state, however, does not appear in AGNRs. Fujita *et al.* have calculated the energy band structure for ZGNRs and AGNRs by using tight-binding approximations (TBA) for the π -states of carbon.¹⁰ They have found that when the width (W) of graphene ribbon is $3n-1$, where n is an integer, AGNR is metallic; otherwise it is semiconducting. However, the first-principles calculations have shown that the hydrogen passivated AGNRs always have nonzero and direct band gaps at the local (spin) density approximation level.¹⁵ The energy gaps (E_g) of AGNRs as a function of ribbon width are classified into three families, in which $E_g(W=3n+1) > E_g(W=3n) > E_g(W=3n+2)$.¹⁵

The capability to control GNRs' electronic properties are highly desired to build future nanodevice directly on GNRs. For example, the electronic structures of AGNRs can be altered through the chemical edge modification.¹⁶ Another possible effective way is to apply external strain, since previous studies have indicated that the uniaxial strain affected significantly the electronic properties of nanoscale carbon material.^{17,18,19} Existing theoretical works focus on electronic structure and magnetic properties of GNRs,^{20,21} nevertheless, more attention should be paid to the geometric deformation effect. In this paper, we perform *ab initio* calculation about strain effect on the electronic structure of AGNRs with various widths. Theoretical results show that the energy gaps can be tuned effectively by external strain. The tunable width of energy gap decreases when the width of AGNRs increases. The nearest neighbor hopping integrals between π - orbitals of carbon atoms are responsible for the variation of energy gap under uniaxial strain.

We apply density functional theory with generalized gradient approximation (GGA) implemented with the DMol³ package.²² The Becke exchange gradient correction and the Lee-Yang-Parr correlation gradient correction are adopted.²³ The basis set consists of the double numerical atomic orbitals augmented by polarization functions. The calculations are all-electron ones with scalar relativistic corrections. Self-consistent field procedure is carried out with a convergence criterion of 5.0×10^{-5} atomic units (a.u.) on the energy and electron density. Geometry optimizations are conducted with convergence criterions of 5×10^{-3} on the gradient, 5×10^{-3} on the displacement, and 5×10^{-5} a.u. on the energy. Medium grid mesh points are employed for the matrix integrations, the real-space global cutoff radius of all atoms is set to be 5.5 Å, and uniformly 22 K points along the one dimensional Brillouin zone are used to calculate electronic structures of the AGNRs.

Here, AGNRs with widths $W=12, 13,$ and 14 are chosen to represent three typical families (corresponding to $3n, 3n+1,$ and $3n+2,$ respectively), similar to the previous theoretical study.¹⁵ As an example, the schematic of an AGNR with width $W=13$ is shown in Figure ???. To avoid the effects of the σ electronic states near the Fermi level, the dangling bonds of edge carbon atom are saturated by one hydrogen atom. All atomic positions of AGNRs atoms are allowed to relax by using a rectangular supercell, in which AGNR is set with its edge separated by at least 10 Å from neighboring AGNRs. As a benchmark, the electronic structures of AGNRs without geometric deformation are calculated. The calculated energy gaps are 0.55, 0.90, and 0.19 eV for the AGNR with width $W=12, 13,$ and $14,$ respectively, which reproduce the previous DFT results.¹⁵

To investigate the electronic structures of these uniaxial deformed AGNRs, the deformation of AGNRs is quantified by the strain (ε) defined as $\varepsilon=(r-r_0)/r_0$, where r and r_0 ($r_0=4.287$ Å) is the deformed and initial equilibrium lattice constant along the axial direction of AGNRs, respectively.²⁴ The electronic structures of the deformed AGNRs with three different widths are all calculated. The band structures for AGNR with width $W=13$ under five different uniaxial strains are shown Figure ??(a), where $\varepsilon=-4.0\%, -0.8\%, 3.0\%, 7.3\%,$ and 10.0% labeled with A, B, C, D, and E, respectively. Note that B and D correspond to two turning points (the maximal and minimal energy gaps), while A, C, E are three intergradation points. Clearly, they exhibit direct band gaps at Γ point for all cases. The obvious difference among band structures of the deformed AGNRs under five different given ε values is the positions of two upmost valence subbands (v1 and v2) and two lowest con-

duction subbands (c1 and c2) relative to the Fermi level. When the applied strain (ε) is set to be -4.0 %, all subbands (v1, v2, c1, and c2) are separated at Γ point. At the maximal energy gap point, we observe that two valence subbands (v1 and v2) and both conduction subbands (c1 and c2) degenerate when the geometric deformation is about -0.8%. These subbands are separated again when further elongating the AGNR up to 3.0 %. When the strain increases continually to 7.3 % (corresponding to the minimal energy gap point), the subband v1 shifts upwards while c1 moves down to the Fermi level, leading these two subbands almost degenerate. When ε further increases to 10.0 %, four subbands are separated again.

We further investigate their electronic properties and observe an interesting phenomenon. The spatial distributions of these subbands (v1, v2, c1, or c2) of the deformed AGNRs with given ε are plotted in Fig. 2 (c)-(d). For A ($\varepsilon=-4.0$ %) case, the valence subband v1 is mainly contributed by the parallel axial bonds, while v2 is featured by the vertical axial bonds. At the turning point B ($\varepsilon=-0.8$ %), it is clear that two subbands (v1 and v2) degenerate at Γ point and their spatial distributions are swapped as seen in Fig. ?? (b). As increasing the strain to 3.0 %, the spatial distributions of c1 and c2 are interchanged as illustrated in Fig. ?? (c). Comparing with spatial pattern at D ($\varepsilon=7.3$ %), this phenomenon happens to two subbands c1 and v1 at E ($\varepsilon=10.0$ %) as shown in Fig. ??(d).

To display more clearly, the variations of energy gap of AGNRs with width $W=12, 13,$ and 14 as a function of ε are shown in Figure ??(a) with filled square, circle, and triangle symbol lines, respectively. The calculated maximal values of E_g for the AGNR with widths $W=12, 13,$ and 14 are 1.07, 1.00, and 0.97 eV appearing at $\varepsilon=5.0\%, -0.8\%,$ and 9.5% , respectively, while the minimal values of E_g are 0.02, 0.03, and 0.03 eV, which occurs at $\varepsilon=-4.5\%, 7.3\%,$ and 1.3% . Although the exact semiconductor-to-metal transition does not achieve by both elongating and compressing the AGNRs, it is clear that the value of energy gap is sensitive to the applied strain (ε). In other words, the uniaxial strain strongly affects the electronic structures of AGNRs. This implies that AGNRs can be used to design as strain sensor. It is interesting to note that the shapes of calculated curves display zigzag feature for three different ribbon widths. The energy gaps change almost linearly between two neighboring turning points by changing the ε .

The variations of the energy gaps of three family structures with different widths ($W=3n, 3n+1,$ and $3n+2,$ where $n=4, 5,$ and 6) as a function of ε are shown in Fig. ?? (b), (c), and

(d), respectively. Obviously, there exist following four main common features for all AGNRs. (1) The zigzag feature is observed for the deformed AGNRs with large width; (2) The energy gap decreases when the width of AGNRs increases without geometric deformation; (3) The minimal energy gap of all deformed AGNRs is several meV, while the maximal energy gap is sensitive to the width of the deformed AGNRs and its value reduces as increasing the width of AGNRs. For example, for the deformed AGNRs with width $W=3n$ ($n=4, 6,$ and 8), the maximal values of energy gaps are 1.07, 0.74, and 0.56 eV, which appear at $\varepsilon=9.5\%$, 6.6% , and 4.8% , respectively, as shown in Fig. ?? (b). (4) Clearly, the distance between between two turning points becomes shorter when the width of AGNRs increases, which suggests that the tunable window of energy gap becomes narrow for the wider AGNRs.

In general, only including a constant nearest neighbor hopping integral (t) between π -electrons TBA results of AGNRs are different from these by first-principles calculations.¹⁵ However, it could reproduce the DFT results of hydrogen passivated AGNRs through introducing of an additional edge hopping parameter.^{15,16} Here, to capture a clearer picture, the electronic structures of the deformed AGNRs are also calculated using the TB model. According to the geometric optimized results, we find that there are four kinds of carbon-carbon bond length in the deformed AGNRs, as labeled by a_n ($n=1$ to 4) in Fig. ??, where a_1 and a_2 stand for the inner C-C distances, while a_3 and a_4 describe the edge C-C separations. The variation of four kinds of bond lengths as a function of the strain ε are shown in Fig. ??(a) for the deformed AGNRs with width $W=13$. Similar results are obtained for AGNRs with width $W=12$ and 14 . It is clear that the C-C separations change almost linearly with the strain and the deformation leads to the largest change of the inner C-C bond length (a_1). The change of C-C distance results in variation of the hopping parameter between two neighbor carbon atoms (t) change in the deformed AGNRs. For simplicity, we assume that the change of t (Δt) is proportional to Δa linearly. Comparing with the change of t_1 (Δt_1), the changes of other three hopping integrals are set to $\Delta t_2=0.15\Delta t_1$, $\Delta t_3=0.40\Delta t_1$, and $\Delta t_4=0.13\Delta t_1$, respectively. The coefficient before Δt_1 is determined by the relative slope as shown in Fig. ?? (a). Four initial hopping parameters for the equilibrium AGNRs without deformation are set to be: $t_1=-2.7$ eV, $t_2=-2.65$ eV, $t_3=-3.2$ eV, and $t_4=-2.75$ eV. The changes of energy gaps of AGNRs versus t_1 are shown in Fig. ?? (b). Clearly, the TBA results reproduce the main feature of DFT calculations. This result shows that the electronic structures of AGNRs can be described by introducing the hopping

parameter t_1 in TB scheme. The change of the hopping parameters of the deformed AGNRs are responsible for the variation of energy gaps.

Recently, Han *et al.* have measured the size of the energy gap of graphene nanoribbons with various widths from 10 to 100 nm.²⁵ They found that the energy gap scales inversely with the ribbon width. Here, we extend the TBA calculations to get the variation of maximal value of E_g as a function of the width of AGNRs (W), as shown in Fig. ?? (c). It is clear that $E_{g_{max}}$ decreases smoothly as increasing the width of AGNRs, which is independent of the family structures. By fitting the calculated curve, we obtain a simple empirical formula, $E_{g_{max}}$ (eV)=14.06/ W , as plotted in Fig. ?? (c) with the green line. We find that this scaling relationship can be used to calibrate the maximal energy gap of AGNRs with large width. For example, the maximal value of energy gap of AGNR with $W=100$ (about 12 nm) is found to be 0.14 eV from TB calculation, remarkably, this empirical relation curve gives the value of 0.14 eV as well. This result also agrees well with the reported experimental value of the GNR without geometric deformation.²⁵

In summary, the electronic structures of deformed AGNRs are calculated by using *ab initio* methods and TB methods. The energy gaps of AGNRs are predicted to change with zigzag shape as a function of the applied strain. The tunable window of the energy gap becomes narrower when the width of ANGRs increases. TBA simulations reproduce these results by first-principles calculations. We find that the change of hopping integrals between π -orbitals of carbon atoms are responsible for the variation of the energy gap of deformed AGNRs. These findings are helpful to construct and design graphene nanoelectronic devices in the near future.

The authors would like to thank Haibin Su for his discussions. This work was partially supported by the National Natural Science Foundation of China under Grand Nos. 10674121, 20533030, 10574119, and 50121202, by National Key Basic Research Program under Grant No. 2006CB922004, by the USTC-HP HPC project, and by the SCCAS and Shanghai Supercomputer Center.

* Corresponding author. E-mail: jlyang@ustc.edu.cn

¹ H. W. Kroto, J. R. Heath, S. C. O'Brien, R. F. Curl, and R. E. Smalley, *Nature* **318**, 162 (1985).

- ² S. Iijima and T. Ichibashi, *Nature* **363**, 603 (1993).
- ³ K. S. Novoselov, A. K. Geim, S. V. Morozov, D. Jiang, M. I. Katsnelson, I. V. Grigorieva, S. V. Dubonos, and A. A. Firsov, *Nature (London)* **438**, 197 (2005); K. S. Novoselov et al., *Proc. Natl. Acad. Sci. U.S.A.* **102**, 10451 (2005).
- ⁴ T. Matsui, H. Kambara, Y. Niimi, K. Tagami, M. Tsukada, and Hiroshi Fukuyama, *Phys. Rev. Lett.* **94**, 226403 (2005).
- ⁵ Y. Zhang, Z. Jiang, P. Small, M. S. Purewal, Y. W. Tan, M. Fazlollahi, J. D. Chudow, J.A. Jaszczak, H. L. Stormer, and P. Kim, *Phys. Rev. Lett.* **96**, 136806 (2006).
- ⁶ Dmitry A. Abanin, Patrick A. Lee, and Leonid S. Levitov, *Phys. Rev. Lett.* **96**, 176803 (2006).
- ⁷ C. L. Kane and E. J. Mele, *Phys. Rev. Lett.* **95**, 226801 (2005).
- ⁸ Y. Zhang, Y. Tan, H. L. Stormer, and P. Kim, *Nature (London)* **438**, 201 (2005).
- ⁹ J. Tworzydło, B. Trauzettel, M. Titov, A. Rycerz, and C. W. J. Beenakker, *Phys. Rev. Lett.* **96**, 246802 (2006).
- ¹⁰ M. Fujita, K. Wakabayashi, K. Nakada, and K. Kusakabe, *J. Phys. Soc. Jpn.* **65**, 1920 (1996).
- ¹¹ C. Berger, Z. Song, X. Li, X. Wu, N. Brown, C. Naud, D. Mayou, T. Li, J. Hass, A. N. Marchenkov, E. H. Conrad, P. N. First, and W. A. de Heer, *Science* **312**, 1191 (2006).
- ¹² Y. Kobayashi, K. Fukui, T. Enoki, K. Kusakabe, and Y. Kaburagi, *Phys. Rev. B* **71**, 193406 (2005).
- ¹³ Y. Niimi, T. Matsui, H. Kambara, K. Tagami, M. Tsukada, H. Fukuyama, *Appl. Surf. Sci.* **241**, 43 (2005).
- ¹⁴ S. Banerjee, M. Sardar, N. Gayathri, A. K. Tyagi, and B. Raj, *Phys. Rev. B* **72**, 075418 (2005).
- ¹⁵ Y. W. Son, M. K. Cohen, and S. G. Louie, *Phys. Rev. Lett.* **97**, 216803 (2006).
- ¹⁶ Z. F. Wang, Q. X. Li, H. X. Zheng, H. Ren, H. B. Su, Q. W. Shi, and J. Chen, *Phys. Rev. B* **75**, 113406 (2007).
- ¹⁷ R. Heyd, A. Charlier, and E. McPae, *Phys. Rev. B* **55**, 6820 (1997).
- ¹⁸ L. Yang and J. Han, *Phys. Rev. Lett.* **85**, 154 (2000).
- ¹⁹ T. Ito, K. Nishidate, M. Baba, and M. Hasegawa, *Surf. Sci.* **514**, 222 (2002).
- ²⁰ N. M. R. Peres, F. Guinea, and A. H. Castro Neto, *Phys. Rev. B* **73**, 125411 (2006).
- ²¹ K. Wakabayashi, M. Fujita, H. Ajiki, and M. Sigrist, *Phys. Rev. B* **59**, 8271 (1999)
- ²² Dmol³ is a density-functional-theory-based package with atomic basis distributed Accelrys. [B. Delley, *J. Chem. Phys.* **92**, 508 (1990).]

- ²³ A. D. Becke, Phys. Rev. A **38**, 3098(1988); C. Lee, W. Yang, R. G. Parr, Phys. Rev. B **37**, 785 (1988).
- ²⁴ The maximal value of the external strain is estimated to be about 20 % through the elastic of two-dimensional carbon plane and the force to break the C-C covalent bond is about 4.0 nanonewtons [E. Konstantinova *et al.*, Phys. Rev. B **74**, 035417 (2006); M. Grandbois *et al.*, Science **283**, 1727 (1999)]. In our calculation, the largest value of the strain ε is about 10%. It means that these AGNRs are stable.
- ²⁵ M. Y. Han, B. Özyilmaz, Y. Zhang, and P. Kim, arXiv:cond-mat/0702511 (2007)

Figure 1: (Color online) Schematic of an AGNR with width $W=13$. Here, the one dimensional unit cell distance between two dash-dotted lines is represented by r . The blue atoms denote hydrogen atoms passivate the edge carbon atoms (black dots). Four kinds of carbon-carbon bond lengths are labeled with a_1 to a_4 .

Figure 2: (Color online) (a) Band structures of AGNRs with the width $W=13$. Here, the uniaxial strain (ε) is set to be -4.0, -0.8, 3.0, 7.3, and 10.0 % and labeled with A, B, C, D, and E, respectively. (b), (c) and (c) The spatial distribution of these subbands (v_1 , v_2 , c_1 , and c_2) near Fermi level of the deformed AGNRs with different strains.

Figure 3: (Color online) Variation of the energy gaps (E_g) for the AGNRs with width $W=12$, 13, and 14 as a function of the strain (ε). Variation of E_g as a function of ε for three family structures with different widths, (a) $W=3n$, (b) $W=3n+1$, and (c) $W=3n+2$ ($n=4$, 6, and 8.)

Figure 4: (Color online) (a) Four kinds of C-C bond lengths of the deformed AGNRs with width $W=13$ as a function of ε . (b) The Variation of the band gap obtained by TBA method for AGNRs with $W=12$, 13, an 14 as a function of the nearest neighbor hopping integral t_1 . (c) The maximal value of energy gap of AGNRs obtained from TBA results versus the ribbon widths with three family structures ($W=3n$, $3n+1$, and $3n+2$, n is a integer).

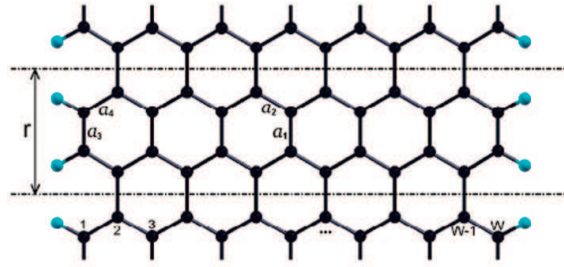


Fig. 1 of Sun *et al.*

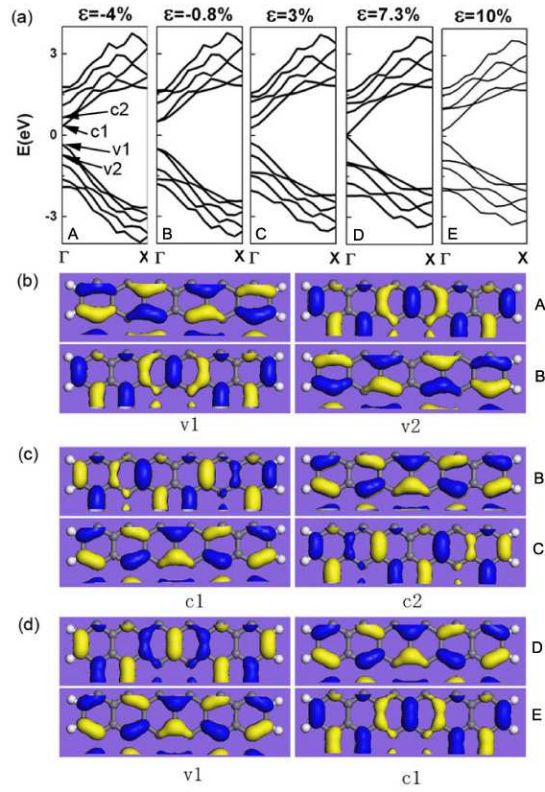


Fig. 2 of Sun *et al.*

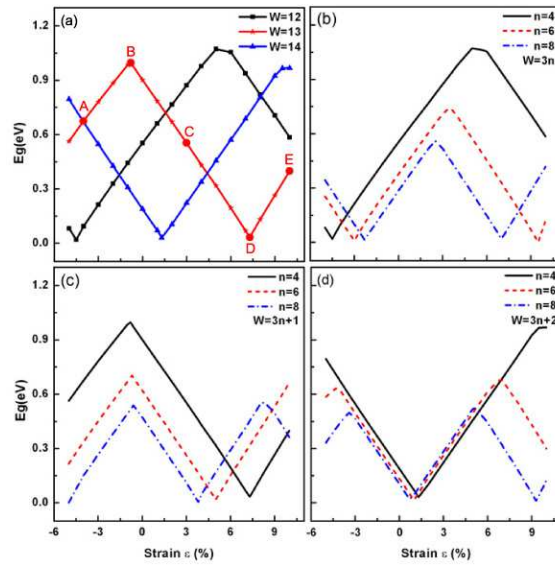


Fig. 3 of Sun *et al.*

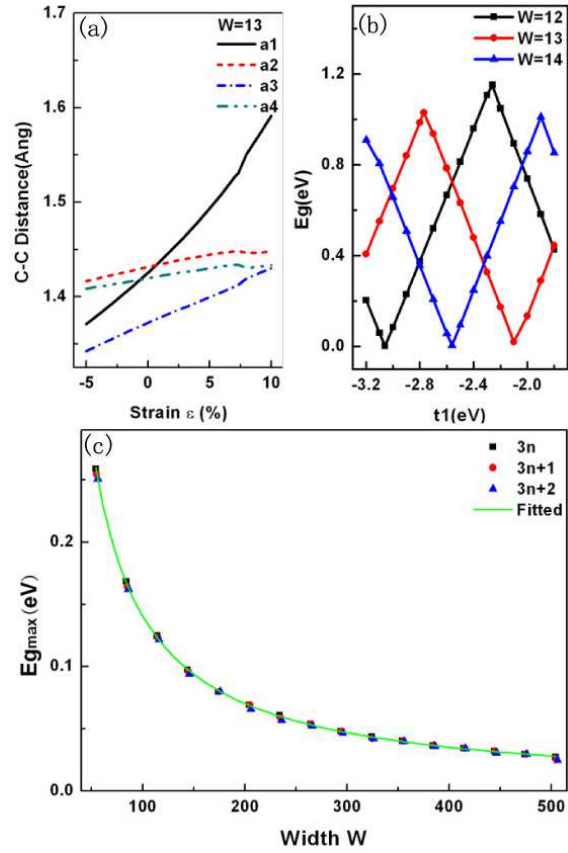


Fig. 4 of Sun *et al.*